

Determining the Influence of Building Density on Heat Island Effect Using Baidu Map and Remote Sensing

Shili Chen, Wei Lang, Xun Li, Chong Shen and Qi Fan

Abstract

This study investigated central urban area of Guangzhou as an example. Data on the types of land use in 2000 - 2009 and building data were used to analyze the changes in the intensity of urban heat island (UHI) by using the meteorological and numerical weather and research forecasting (WRF) model. The correlation analysis method was used to analyze the temperature and building density to explore the decisive influence of building density on the UHI effect. Results showed that the WRF model can be used to simulate the temperature and humidity performance in the UHI effects. Moreover, urban building density have a great coefficient with UHI. The UHI effect is relatively weak when a few buildings sparsely distributed, various building densities have a substantial influence on the UHI effect. In general, urban development in Guangzhou has enhanced human activities and changed the type of land use, thereby considerably influencing the UHI effect.

Introduction

Given the rapid development of urbanization and industrialization, the considerable heat island effect has substantially affected the daily lives of urban residents and the urban ecological environment worldwide. Urban heat island (UHI) is a typical representative of urban change caused by urbanization. UHI is the phenomenon, in which the urban surface and atmospheric temperature are higher than those of the surrounding non-urban environment; this phenomenon is caused by land use, thermodynamic power, and release of human heat, which are considerably common in metropolitan areas (Oke, 1982; Buyantuyev and Wu, 2010).

Lake Howard, a British climate scientist, first recorded the phenomenon in 1833 in his book *London Climate*, in which the main idea is that the temperature in the city center is higher than that in the suburbs. This climate characteristic is known as the “heat island effect” (Luke, 1818). Manley proposed the concept of UHI for the first time in 1958 (Mnaley, 1958). Four methods are commonly used to detect the heat island effect, namely, point observation, numerical simulation, meteorological data, and remote sensing research methods. In particular, the extensiveness of the observational data and the development of remote sensing technology have expanded the method from point to surface and have obtained the research results on the phenomena and laws of the UHI effect (Unwin, 1980). Simultaneously, laboratory development (Cenedese,

2003) and numerical simulation (Kusaka, 2000) further promoted the study of the UHI effect.

In recent years, many scholars mainly focused on the shape and structure (Miao *et al.*, 2009), energy change (Champollion *et al.*, 2009; Ryu and Baik, 2012), interaction mechanisms, and simulations (Freitas *et al.*, 2007; King and Davis, 2007) in the heat island research of cities. The scholars determined that urbanization has changed the atmospheric dynamics and heat exchange properties of underlying surfaces. Moreover, surface cover and land use have changed rapidly, thereby promoting the formation of UHI. In particular, many scholars have emphasized that changes in land use and vegetation cover are the major factors in the formation and evolution of the UHI effects (Kolokotroni and Giridharan, 2008). Each type of land use has different thermal or radiological characteristics and is often characterized by high temperature for urban land use, whereas natural elements (e.g., bare soil, vegetation, and water) have cooling effects (Sun, 2012; Sun *et al.*, 2012). Thus, the expansion of cities causes changes in the type of land use, thereby resulting in a corresponding change in the UHI effects. Data on changes in the type of land use were obtained using remote sensing images. The simulation of heat island strength using the weather and research forecasting (WRF) model is still relatively limited.

Many scholars believed that the pattern, structure, and material composition of an urban space are closely related with heat island (Connors *et al.*, 2013; Wu, 2014). Zhang *et al.* (2008) considered that no rational allocation of various types of surface composition on landscape structure caused the formation of heat island; thus, urban planning and design, which consider the elements of landscape pattern, is based on the overall macro of a city (Guo *et al.*, 2015; Kuang *et al.*, 2015; Zhang *et al.*, 2008; Zhang *et al.*, 2013; Zhou *et al.*, 2011). In recent years, the renovation of the urban construction layout has changed the original natural landscape because of the rapid progress of urbanization and the real estate industry in China. The rapid increase of the volume and building density in the urban construction area become the major factor that affects the heat island effect. Building density, which indicates the ratio of the coverage of the buildings' footprints to the size of the area of interest (Zhang *et al.*, 2017), relatively reflects the building-intensive and empty rate, as well as the living environment, traffic, green conditions, and ecological environment, of the city. Moreover, numerous scholars have used remote sensing data to extract urban building information (Huang and Zhang, 2012; Huang *et al.*, 2014; Hussain *et al.*, 2013). In the process of rapid urbanization, urban

Shili Chen, Wei Lang, and Xun Li are with the Department of Urban and Regional Planning, Sun Yat-sen University, Guangzhou 510275, China; and the Urbanization Institute of Sun Yat-sen University, Guangzhou 510275, China (lixun@mail.sysu.edu.cn; lixun23@126.com).

Chong Shen and Qi Fan are with the School of Atmospheric Sciences, Sun Yat-sen University, Guangzhou 510275, China.

Photogrammetric Engineering & Remote Sensing
Vol. 84, No. 9, September 2018, pp. 549–558.
0099-1112/18/549-558

© 2018 American Society for Photogrammetry
and Remote Sensing
doi: 10.14358/PERS.84.9.549

construction has gradually replaced the original surface types, such as natural vegetation and wetland, thereby resulting in the gradual increase of the regional mean land surface temperature (LST). Furthermore, the spatial distribution of the UHI area is substantially concentrated. The results show that surface temperature is positively correlated with the density distribution of urban buildings. Moreover, large building density results in a substantial heat island effect. Therefore, the rational control and improvement of an urban building layout is conducive in reducing the heat island effect.

This research is based on 3S (Remote Sensing, Global Position System, Geographic Information System) technology, high precision map, and remote sensing data using ArcGIS® 10.5 and ENVI 5.1 software and taking Guangzhou as the example. First, the temperature and humidity of the heat island effect is simulated and analyzed using the data on land use from 2000 and 2009 and considering the high-resolution WRF model, which was developed by the National Atmospheric Research Center (NCAR). Furthermore, the quantitative method is used to detect the relationship between building density and heat island effect and their time-varying characteristics and mechanisms. The current study shows that the intensity of the heat island increases with the development of the urbanization process (Lang *et al.*, 2016a; Sobstyl *et al.*, 2018). The heat island intensity during summer is substantially higher than that during winter. The relationship between building density and heat island strength indicates that building density has an important effect on heat island strength. This study also emphasizes that the influence of urban building density distribution on the UHI effect can provide a scientific basis for urban planning and thermal environment management.

Research Area and Data

Research Area

As the research object in this study, Guangzhou is in southern China, the northern edge of the Pearl River Delta, and brink of China's South Sea across Hong Kong and Macao. Meanwhile, Guangzhou is also called China's "South Gate" Metropolitan area and is the starting point of Silk Road. In the past 20 years, the urban built-up area has expanded from 553.5 km² in 2002 to 1237.25 km² in 2015 because of the rapid progress of urbanization and expansion. Furthermore, urban buildings continue to upgrade and the heat island effect is also increasing because of the rapid development of urban construction (Lang *et al.*, 2016b). Therefore, investigating the relationship between building density and heat island intensity in the main urban area of Guangzhou is necessary. The research area (see Figure 1) includes the districts of Liwan, Yuexiu, Tianhe, and Haizhu, which are surrounded by the Pearl River and have a total land area of 376.37 km².

Data

This research uses the spatial distribution data of the urban building density and the remote sensing data of the land use change model to simulate the heat island effect. Building density is known as the building coefficient, which denotes the ratio of the base area to the land area of all buildings in a certain range of land use. Building density is an important indicator of land intensity and can also reflect the vacancy rate. The urban building footprint spatial distribution data of this study is obtained by crawling from the Baidu map, which contains the shape of each building within the city (see Figure 2a). The building density is shown in Figure 2b.

The global land cover data, namely, GLC2000 and GLC2009, are obtained from the Système Probatoire d'Observation de la Terre (SPOT) satellites and Envisat satellites in 2000 and 2009, respectively. These data have a spatial resolution of 1 km and 300 m, respectively, and the classification criteria are from the land cover classification system (LCCS) (see Figure 3). Nov 2024 08:24:17

Copyright: American Society for Photogrammetry and Remote Sensing

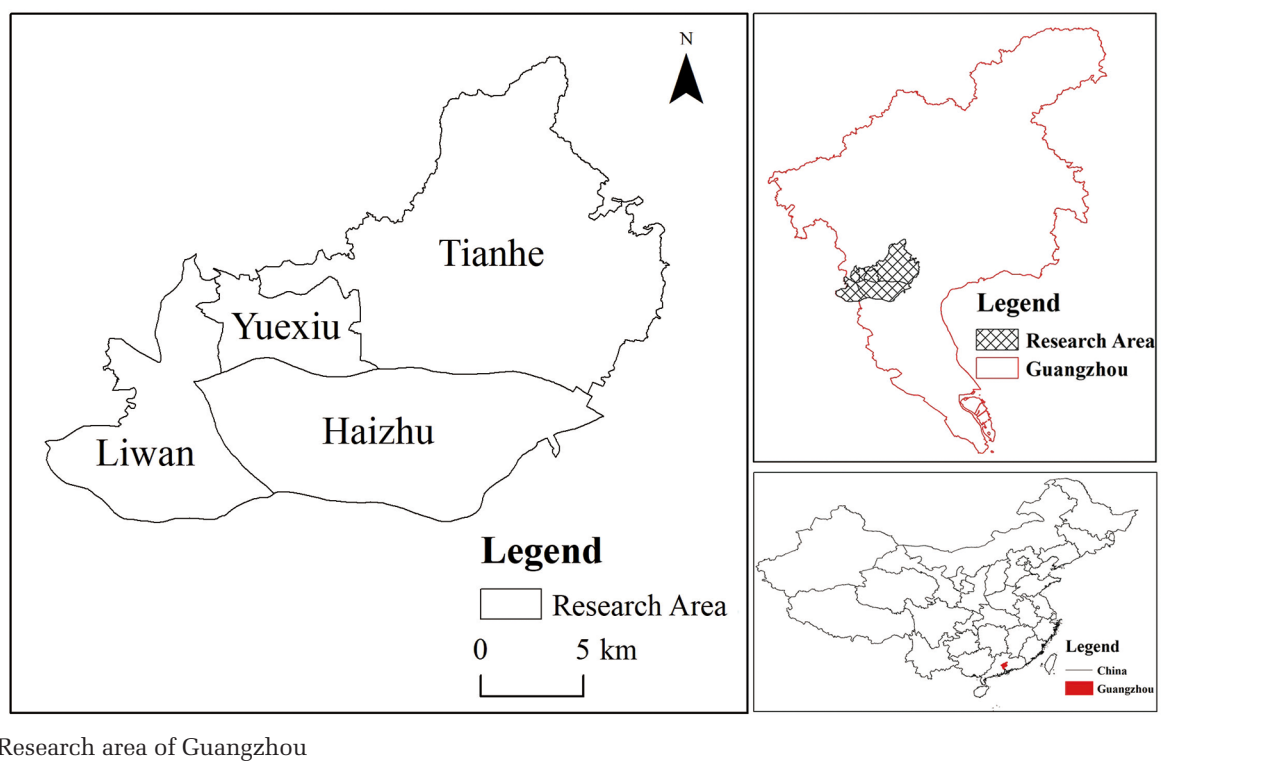


Figure 1. Research area of Guangzhou



Figure 2(a). Building footprint of the research area

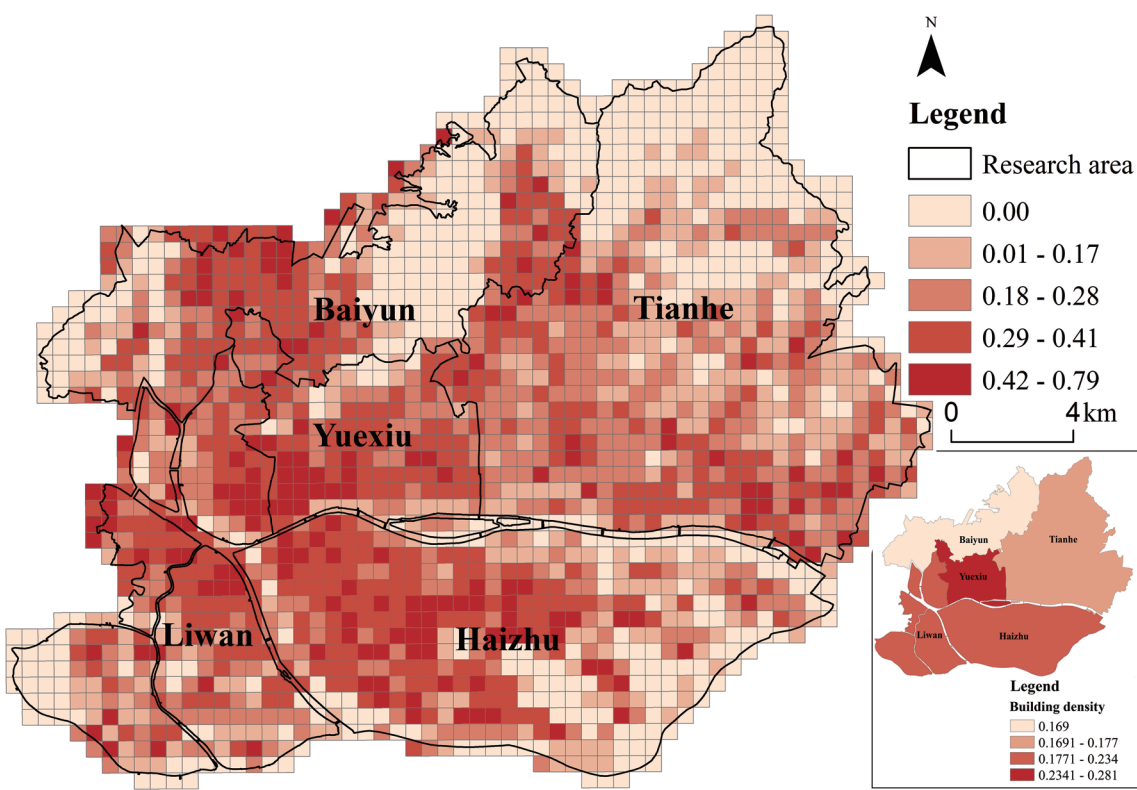


Figure 2(b). Building density of the research area

Methodology and Theory

WRF Model

The WRF model is a high-resolution weather research and forecast model developed by NCAR and is an extensively used

meteorological model. In recent years, many related outcome in the study of urban effects have been conducted using this model (Masson, 2006). This model has a considerable effect on various terrain and multiple nested networks because it

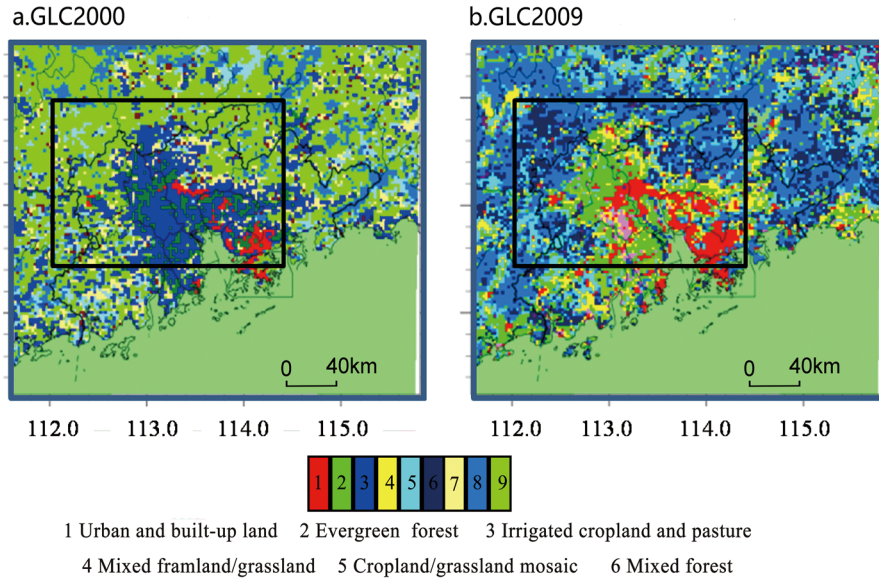


Figure 3. Spatial distribution of land use types in the Pearl River Delta: (a) GLC2000; (b) GLC2009

Table 1. Comparison of the simulated and observed temperature, relative humidity, and wind speed.

	Elements	OBS	SIM	MB	MAE	RMSE	R	IOA
January	Rh2 (%)	76.43	73.19	-3.24	6.23	7.49	0.87	0.99
	T2 (°C)	14.79	16.45	1.66	2.39	2.84	0.80	0.99
	WS10 (m/s)	1.71	2.43	0.72	0.91	1.17	0.60	0.92
	Rh2 (%)	74.01	74.96	0.95	6.49	7.71	0.66	0.99
July	T2 (°C)	29.21	29.69	0.48	1.37	1.71	0.75	0.99
	WS10 (m/s)	2.12	2.63	0.51	1.31	1.76	0.67	0.88

adopts advanced numerical calculation and data assimilation technology. In particular, the WRF model has been extensively used in simulation theory and the application of the heat island effect. Accordingly, the WRF model is an important mesoscale numerical model in the study of the heat island effect.

This study simulates the temperature and humidity of Guangzhou in 2000 and 2009 using the WRF meteorological model, which uses two types of land use type data from various times and sources of remote sensing image. The changing characteristics of the heat island effect in Guangzhou over time are analyzed as well.

Experimental Design of Simulation

The WRF model is used as a research tool to design a four-nested grid with a Lambert map projection. The horizontal lattice is 27, 9, 3, and 1 km. The simulation results of the fourth grid in the main urban area of Guangzhou are analyzed. The vertical layer has 30 layers and the top of the model is 50 hPa. A set of parameters for the Pearl River Delta region are summarized by referring to the relevant research on the numerical simulation of WRF in this region. The model uses the two-moment cloud microphysical scheme (WRF Double-Moment 6-Class, WDM 6).

Monin–Obukhov surface layer parameterization scheme, Noah L and Surface Model, and YSU planetary boundary layer scheme. The Kain–Fritsch cumulus scheme is employed in the simulation regions D01 and D02. No cumulus convection parameterization scheme is used in the simulation regions D03 and D04, because the grid can't distinguish cloud-scale physical quantities. The initial and boundary conditions are

provided by $1^\circ \times 1^\circ$ FNL reanalysis data every 6 h and interpolated into the simulation area.

In addition, two simulated tests are set up in January and July. The simulation time in January was from 30 December 2009 at 00:00 (universal time coordinated (UTC)) to 01 February, 2010 at 00:00, whereas that in July was from 29 June, 2010 at 00:00 to 01 August at 00:00, which is two days before the starting time (spin up). The January and July control (GLC2009) and sensitivity tests (GLC2000) used the same physical parameters and initial and boundary conditions, in which the only difference is the underlying surface type data. The two sets of underlying surface type data used in the control and sensitivity tests, which are represented as GLC2009 and GLC2000 for 2009 and 2000, respectively, are shown in Figure 3.

Model Validation

The observation data of the Guangzhou, Dongguan, and Gaoyao sites

were selected to test the accuracy of the simulated meteorological field. The main test elements included 2 m temperature, 2 m relative humidity, and 10 m wind speed. Table 1 shows the results of the 2 m temperatures (T2), 2 m relative humidity (Rh2), and 10 m wind speed (WS10) simulated using GLC2009 in January and July (i.e., OBS is the observed average, SIM is the simulated average, MB is the mean deviation, MAE is the average absolute error, RMSE is the root mean square error, R is the correlation coefficient, and IOA is the compliance index). The relative humidity, temperature, and wind speed IOA are above 0.88 in January and July, and the temperature and humidity IOA even reached 0.99 (see Table 1). The simulated result is considerably accurate in January and the correlation coefficient is over 0.8. The simulation result in July is not as good as that in January, although the correlation coefficient is above 0.66. In general, the simulation results can considerably reflect the actual situation of the atmosphere.

Estimation of the Nuclear Density

The sizes of various buildings in different radius ranges vary with the range of the heat source at the center point. A limited number of radius factors are considerably few and a substantially large scale is difficult to add in the calculation of irrelevant objects, thereby increasing the error. This situation requires the best radius, that is, the most sensitive scale that can reflect the building density on the heat island mechanism and range regulation. The nuclear density estimation method is based on the first law of geography (i.e., everything is related to everything else, but near things are more related than distant things). The spatial feature distribution for the depth characteristics of information mining or regular spatial distribution characteristics is an accurate tool for analysis and can be used to assess the size of a building in a specific range based on the magnitude of the heat island size impact.

The principle of nuclear density estimation method is based on point P, threshold r, which is the number of information of a radius within a circle and divided by the area of the circle. The nuclear density of general point P can be expressed as follows:

$$P(x) = \frac{1}{nh} \sum_{i=1}^n \left\{ K \left[\frac{d(x, x_i)}{h} \right] \right\}, \quad (1)$$

where n represents the number of geographic information contained in the distance scale range, $K()$ denotes the kernel density function, $d(x, x_i)$ represents the Euclidean distance between two points, and h denotes the distance threshold, that is, the scale of the nuclear density estimation method. Several studies have shown that threshold h has considerable influence on nuclear density analyses and outcomes. That is, a suitable spatial scale exists. This scale is extremely useful for analyzing the effect of building density on the heat island effect at a certain scale.

Results

Impact of Land Use Change on the UHI Effect

The data of the land use type change in Guangzhou City in 2000 and 2009 are used as bases to analyze the changes of the heat island effect intensity after the land use type change in the main urban area from two aspects, namely, temperature and humidity. Such analysis could reflect the heat island effect intensity.

Temperature Changes

When land use type changes, the geometric, radiological, and thermodynamic parameters of the surface change the surface energy balance, thereby resulting in changes in the near-stratospheric temperatures. The most prominent feature of urbanization is the urban heat island effect. In this study, the simulated 2 m temperature (T_2) by the WRF mode is used to discuss the effect of urban expansion on the temperature during the whole day, daytime, and nighttime.

The comparison of the simulated results for the monthly average temperature in the GLC2000 and GLC2009 cases is shown in Figure 4. The temperature of the main urban area in Guangzhou in GLC2000 case is not substantial. Given the advancement of the urbanization process, the average temperature of the main urban area is substantially higher than those in the other regions, thereby forming a large-scale UHI. The difference in the 2 m temperature between the two tests can well reflect the warming effect caused by urban development.

The difference between GLC2000 and GLC2009 cases shows that the 2 m temperature in the simulated area in January and July increased under various degrees. The average temperature increased by 0.20°C in January and 0.31°C in July. In particular, the Liwan, Yuexiu, and Tianhe districts are the most evident warming regions that form a substantially high-temperature peak area.

The warming effect associated with urban development has an evident diurnal variation before 18 o'clock to reach the maximum. The maximum temperatures for January and July are 1°C and 2.2°C , respectively (see Figure 5). On the one hand, the warming effect of urban development on the atmosphere is apparent at night because the heat storage capacity of a city is higher than that in a farmland. The heat stored during the day will be released at night. On the other hand, the night boundary layer height is low. The vertical exchange of heat is weaker at nighttime than daytime. The amount of heat released from the underlying surface of a city is distributed over a relatively short air column. Thus, the temperature of urban surface increases substantially at night.

Humidity Change

Urban development also has a certain impact on relative humidity. The simulated results of the 2 m relative humidity (Rh_2) by the GLC2000 and GLC2009 cases in the January and July are compared (see Figure 6). The relative humidity in the main urban area was substantially lower than that in the other areas, thereby forming a broad range of urban dry island. From the monthly average 2 m relative humidity differences, the expansion of the underlying surface resulted in a consistent decrease in 2 m relative humidity in the central urban area of Guangzhou in January and July. The monthly average of relative humidity in January and July decreased by 1.14 percent and 2.1 percent, respectively. Relative humidity indicates the moisture level of a block and is affected by the absolute humidity and temperature. In urbanization, extensive areas of arable land have been converted into construction land. Thus, the ground water permeability is decreased, vegetation coverage area is reduced, rainwater is rapidly lost after the rain, and the ground rapidly dries up, thereby resulting in the reduction of the absolute water vapor content of the city. Furthermore, the increase in urban temperature increases the saturated vapor pressure. Thus, the relative humidity decreases.

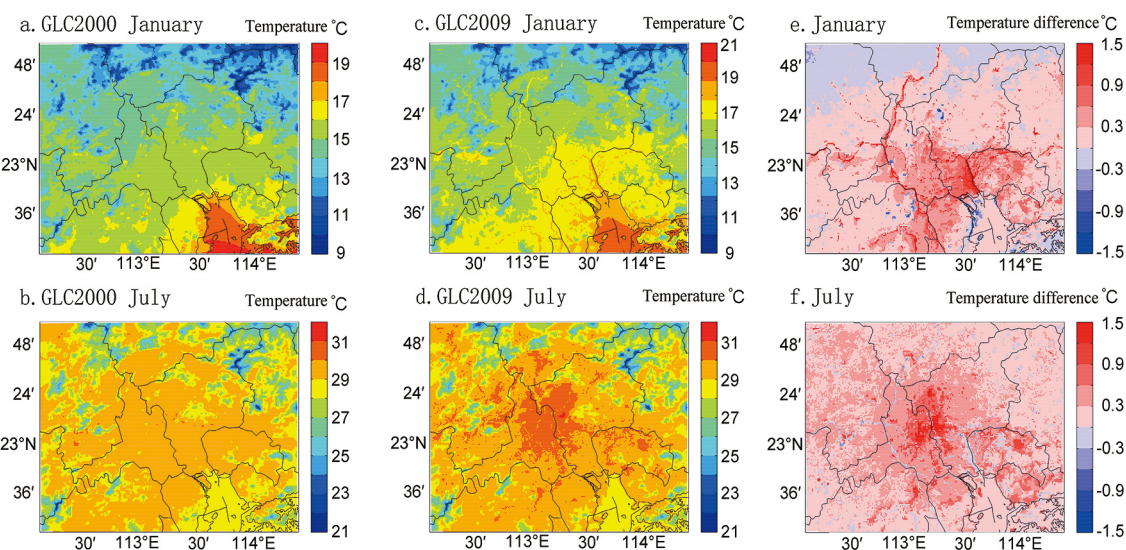


Figure 4. Simulated spatial distribution of monthly average 2 m temperature ($^\circ\text{C}$) in the GLC2000 and GLC2009 cases and the monthly average 2 m temperature differences (differences = GLC2009–GLC2000)

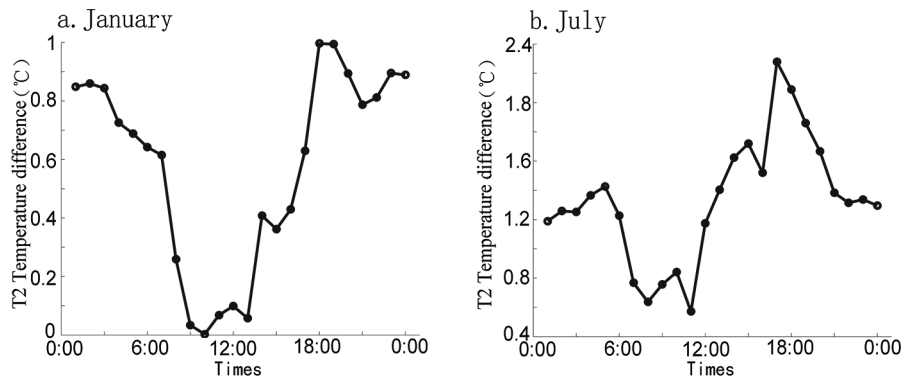


Figure 5. GLC2009 and GLC2000 test simulations of the daily variation of the temperature difference of the 2m curve (a, January; b, July) (difference = GLC2009–GLC2000)

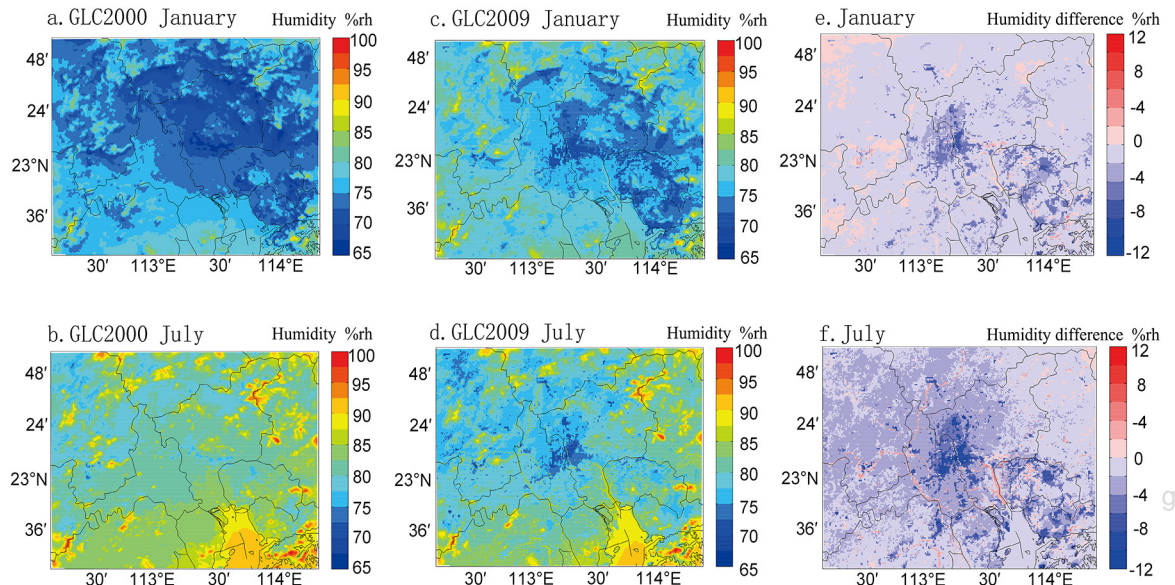


Figure 6. Simulated spatial distribution of monthly average 2 m relative humidity (%) in the GLC2000 and GLC2009 cases and monthly average 2 m relative humidity differences (differences = GLC2009–GLC2000)

Impact of Building Density on Heat Island Strength

Impact of Nuclear Building Density on the Change of Scale

Building density refers to the proportion of the total area occupied by the total floor area of all buildings in a certain area. Previous planning and design are often based on the plot of building density calculation and the actual division of the entire land is uniform, thereby disregarding the spatial location of each point difference. “Nuclear building density” is the ratio of the total gross area to building land area within a certain distance from a specific point in space. The law of spatial autocorrelation suggests the inclusion of a large radius scale range, additional global trends, and large amount of adjacent building foundation in the calculation. When the radius scale range is small, the size of the adjacent building base included in the calculation is also small and the representation becomes substantially localized. In this regard, this study sets a different radius of the search circle and calculates and evaluates the density of the nuclear buildings with the increase of the scale. First, the heat island effect simulation point in the study area is determined. Second, the sensitivity index of various spatial scales is calculated and tested using

Equation 1 from a radius of 100, 150, 200, and 250 m to 700 m. Last, the scale sensitivity curve of the building density and scale is drawn with the calculated results (see Figure 7).

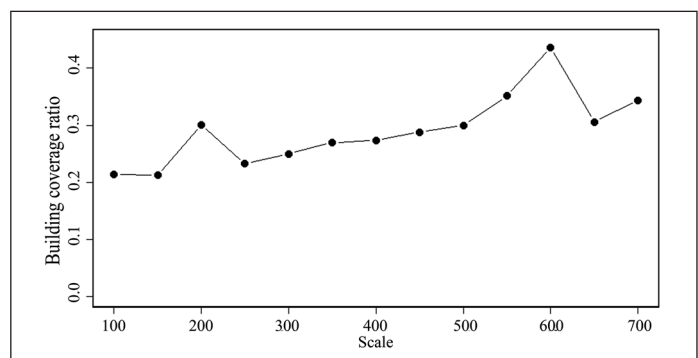


Figure 7. Building coverage ratio of an observation point with various scales

At a radius of 100 m, the building density gradually increases (see Figure 7). At a radius of 600 m, the building

Table 2. Correlation coefficient between building density and temperature/humidity in scale.

Scale (meters)	Humidity between 2000 and 2009 years in January(Rh2)	Temperature between 2000 and 2009 years in January(°C)	Humidity between 2000 and 2009 years in July(Rh2)	Temperature between 2000 and 2009 years in July(°C)
100	0.30	0.22	0.25	0.26
150	0.34	0.27	0.28	0.29
200	0.38	0.32	0.32	0.33
250	0.41	0.36	0.35	0.36
300	0.42	0.38	0.36	0.37
350	0.44	0.39	0.38	0.39
400	0.45	0.40	0.39	0.39
450	0.46	0.41	0.39	0.40
500	0.46	0.41	0.40	0.41
550	0.47	0.42	0.41	0.42
600	0.49	0.43	0.44	0.45
650	0.48	0.42	0.43	0.44
700	0.48	0.41	0.43	0.44
750	0.49	0.41	0.44	0.45
800	0.50	0.42	0.45	0.46
850	0.51	0.42	0.46	0.47
900	0.51	0.43	0.47	0.48
950	0.53	0.43	0.48	0.49
1000	0.54	0.44	0.50	0.50

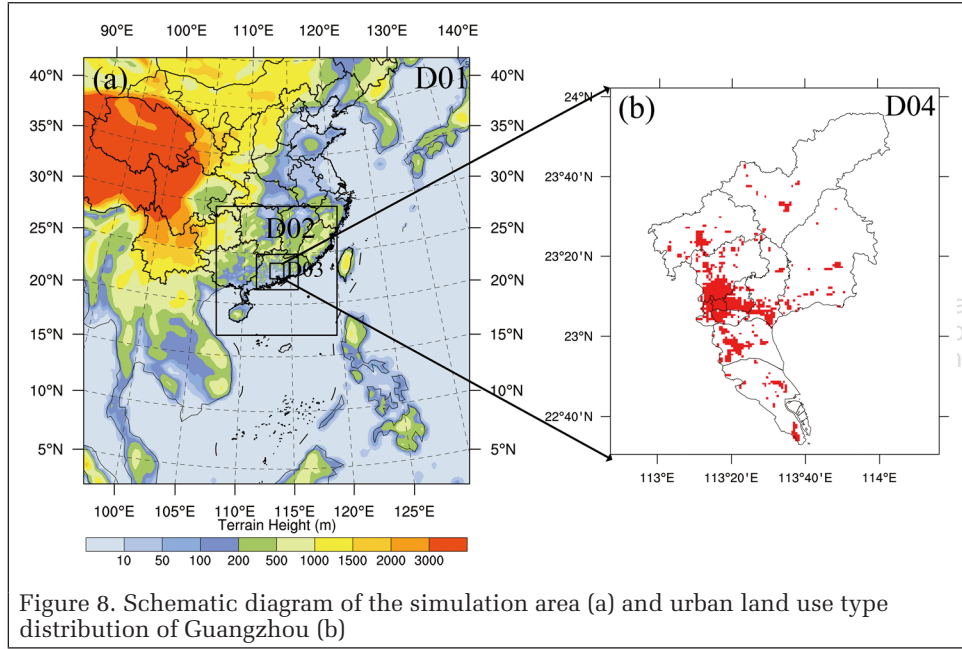


Figure 8. Schematic diagram of the simulation area (a) and urban land use type distribution of Guangzhou (b)

density tends to moderate. Therefore, the nuclear building density in the space search radius of 600 m has the best reflection impact of heat island strength. That is, the building density of the observation point has the maximum impact of heat island strength within a radius of 600 m.

Influence of Nuclear Building Density on Heat Island Strength

The intensity of UHI is mainly reflected in the temperature, humidity, and other changes. Many factors affect intensity change. Therefore, building density is compared with the temperature and humidity in 2000 and 2009 at various scales. Table 2 shows that at the 0.01 significance level, a significant correlation exists between building density and temperature and humidity at various scales. Moreover, the humidity is more apparent than the temperature and the change in January is more intense than in July. Meanwhile, the analysis results show that a slight decrease and gradual increase in the correlation between building density and temperature and

humidity after 600 m are observed. These results are closely related to the change of building density in the change of scale. Building density in the space search radius of 600 m has the best reflection impact on the heat island strength.

The correlation coefficient of temperature and building density in Table 2 is 0.54, thereby indicating the existence of a close, positive correlation. Thus, a high density of urban buildings will result in a high temperature. Numerous urban buildings results in a reduction in wind speed in the area, thereby reducing the air ventilation efficiency in the region. This outcome may be observed without wind in the local area, thereby resulting in a further increase in the regional air temperature. Furthermore, free space is nearly absent in the urban high-density building area as a place of public activity, such as greening and square, and man-made heat is likely to be produced. Hence, the regional heat island effect deteriorates. However, when only a few buildings are present and the distribution is sparse, the exchange of hot and cold air is favorable, air ventilation efficiency is high, and the heat island effect is relatively weak. However, the large distance among buildings in a high-rise building area is favorable for air ventilation efficiency. A high-rise building can appropriately increase the ground shadow area, thereby reducing the cumulative sunshine time in the area. This result reduces the non-building surface acceptance of the solar direct radiation, thereby decreasing the solar radiation generated by the warming.

Discussion

To verify the effects of various building densities on the heat island effect, this study used the buildings (construction area: see Figure 8b) within Guangzhou City as the land use type

for the heat island effect simulation analysis. The ideal sensitivity tests are performed using the WRF mode coupled with the multi-layer urban canopy model (BEP). A total of 30 eta levels with the pressure of 50 hPa at top level are used. The domain uses a grid of 100×110 , 94×100 , 161×136 , and 160×178 with horizontal spatial resolutions of 45, 15, 3, and 1 km, respectively. The most inner domain (D04) covers the entirety of Guangzhou. The simulation area is shown in Figure 8a. The meteorological initial and boundary conditions were derived from the National Centers for Environmental Prediction global reanalysis data of $1^\circ \times 1^\circ$.

Considering the spin-up time, the simulation time is from 00:00 (world time) on 31 October, 2016 to 00:00 on 04 November, while the analysis period is from 00:00 (local time) on 02 November to 23:00 on 03 November. Guangzhou has fine weather during this time period, thereby making

the urban heat island effect apparent. Meanwhile, analyzing the shadowing effect of buildings on solar radiation is easy. Sensitivity tests are mainly used to set the building width and street width in the BEP scheme to represent the density of buildings in the urban underlay area. The details are shown in Table 3. The Base, Case1, and Case2 experiment settings analyze the influence of the three types of building density on the meteorological elements for middle, high, and low. In particular, the Case1 experiment sets the building density higher than that of the Base experiment, whereas the Case2 experiment has a lesser building density than that of the Base experiment.

Table 3. Simulation scheme settings.

Scheme setting	Height distribution (m)	Floor width (m)	Road width (m)	Marks
Base	15(30%), 25(40%), 35(30%)	20	20	Medium density
Case1	15(30%), 25(40%), 35(30%)	10	10	High density
Case2	15(30%), 25(40%), 35(30%)	30	30	Low density

Table. 4 Comparison of the simulated and observed temperature, relative humidity, and wind speed

Elements	OBS	SIM	MB	MAE	RMSE	R
T2 (°C)	20.89	22.15	1.27	1.30	1.58	0.97
Rh2 (%)	60.92	62.79	1.87	3.60	4.10	0.93
WS10 (m/s)	2.09	3.02	0.93	0.93	0.98	0.76

We selected the observation data from 221 automatic weather stations in Guangzhou to test the simulation results and the accuracy of the simulated meteorological field. The main test elements included 2 m temperature, 2 m relative humidity, and 10 m wind speed. The results of T2, Rh2, and WS10, which were simulated using the Base experiment, are shown in Table 4. The deviations of T2, Rh2, and WS10 are simulated and the observed values are 1.27°C, 1.87 percent, and 0.93m/s, respectively (see Table 4). All correlation coefficients are above 0.75 and the correlation of T2 and Rh2 are over 0.93. The comparison of the average T2, Rh2, and WS10 distribution maps simulated using the Base experiment and the observed values of the Guangzhou automatic weather station are shown in Figure 9. The horizontal distribution of the simulation results of all meteorological elements are also consistent with the observations. In the downtown area, the horizontal distribution characteristics of higher temperature, lower humidity, and lower wind speed were particularly

simulated. In general, the simulation results can substantially reflect the actual situation of the atmosphere.

In addition, this research focused on the effects of building density on temperature and analyzed the impact of various building densities on the average 2 m temperature of Guangzhou at daytime (08 to 19 AM) and nighttime (00 to 07 AM, and 20 to 23 PM). In Figure 10 A-a and Figure 10B-d, the temperature of the main urban area in Guangzhou is evidently higher than the other regions, thereby forming a large-scale urban heat island. Liwan, Yuexiu, Tianhe, Haizhu, central Panyu, South Baiyun, and Huangpu districts are particularly warm regions, thereby forming a considerably high-temperature peak area. After changing the building density, the simulated 2 m temperature of each experiment has an apparent effect on the urban underlying surface. At daytime, the high building density (see Figure 10A-b) decreased the temperature of the urban underlying surface by approximately 0.3°C compared with the simulation results of the middle building density (see Figure 10 A-a). The low building density (see Figure 10 A-c) increased the 2 m temperature by approximately 0.18°C. However, the influence of building density on the 2 m temperature at nighttime is opposite to that of daytime. The high building density increased the 2 m temperature of the urban underlying surface by approximately 0.12°C (see Figure 10 B-e). The low building density decreased the 2 m temperature by approximately 0.08°C (see Figure 10B-f). The reasons are that the higher building density makes the street valleys narrower in the same area, the buildings have a clear shadowing effect on the short-wave radiation during the daytime, and the amount of heat that reaches the ground decreases, thereby resulting in a decrease in the 2 m temperature. However, the increase in the width of the street valley (low urban density) increases the amount of heat received by the ground and increases the 2 m temperature. At nighttime, the urban canopy has a significant trap effect on the long-wave radiation because of the narrower street and valley. The heat trapped inside the canopy increases, the 2 m temperature increases, and the wide street valley decreases the amount of heat trapped inside the canopy. Thus, the 2 m temperature also decreases accordingly.

In Figure 10C, the warming effect associated with building density changes has an apparent diurnal variation in Guangzhou. From 08:00 to 19:00, the high building density decreases the 2 m temperature (Case1 - Base), whereas the low building density increases the 2 m temperature (Case2 - Base). The most apparent effect was observed at noon. The 2 m temperature decreases by 0.41°C (at 12 o'clock) and increases by 0.24°C (at 15 o'clock). From 00:00 to 07:00, the high building density increases the 2 m temperature from 0.11°C to 0.18°C. The low building density decreases the 2 m temperature from 0.01°C to 0.07°C. This study shows that the high building

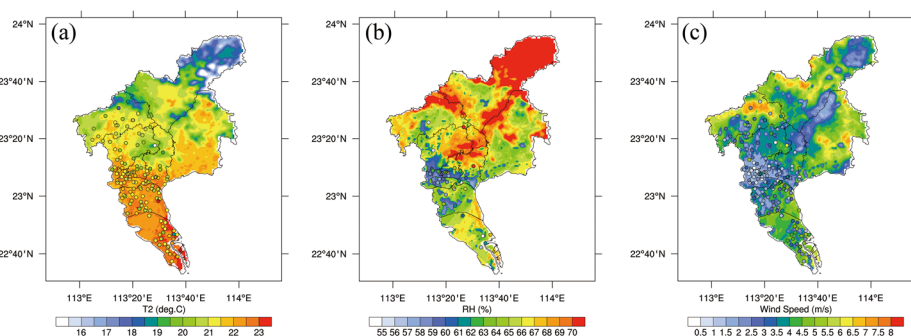


Figure 9. Results of the horizontal distribution of the Base scheme simulation and observations of the Guangzhou automatic weather station (Polka Dots) (a, T2; b, Rh2; c, WS10)

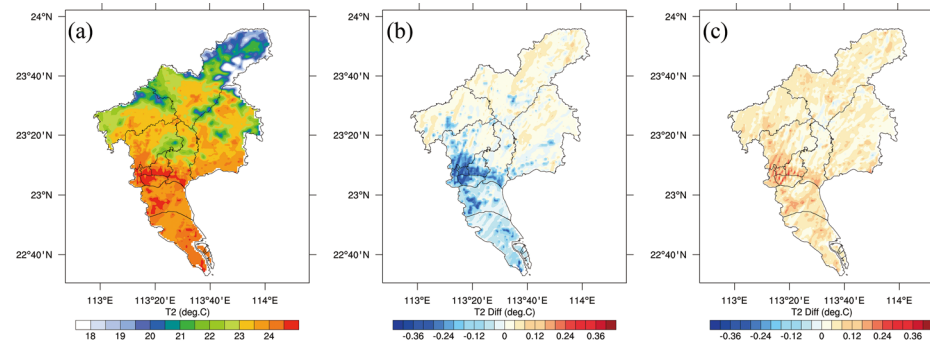


Figure 10(a). Effects of various building densities on the average 2 m temperature (T2) at daytime in Guangzhou (a, Base; b, Case1 and Base; c, Case2 and Base)

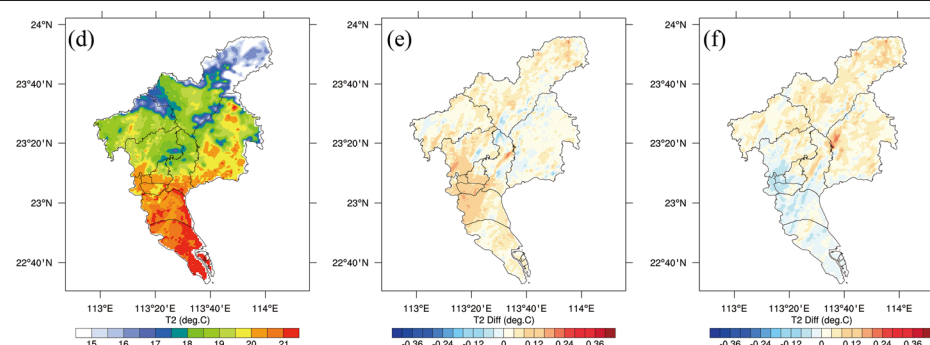


Figure 10(b). Effects of various building densities on the average 2 m temperature (T2) at nighttime in Guangzhou (d, Base; e, Case1 and Base; f, Case2 and Base)

density has a greater impact on the 2 m temperature than the low building density, and the 2 m temperature is more affected at daytime than at nighttime.

Conclusions

The temperature and humidity of the main urban area in Guangzhou were extracted from the land use data in 2000 and 2009 by using the WRF model. The temperature and building density were analyzed using the correlation analysis method. The result shows that diverse human activities brought about by urbanization and change of land use type have an important influence on the heat island effect, thereby mainly showing increasing temperature and humidity in the study area. The change of human activities and land use type pose considerable influences on the heat island effect. The various building densities have a significant influence on the heat island effect.

The temperature and humidity in Guangzhou have a time of volatility and spatial difference. In the past few years, the change of temperature and humidity slightly fluctuated in January and July and the overall trend is increasing. The temperature and humidity changes in the Tianhe and Haizhu districts are apparent, whereas those of the Liwan and Yuexiu districts are insignificant. In particular, the monthly mean temperature in the simulated area in January and July increased by 0.20°C and 0.31°C, respectively. The monthly average relative humidity was significantly lower than that in other areas in the main study area. The relative humidity monthly average decreased by 1.14 percent and 2.1 percent in January and July, thereby forming a broad range of urban dry island. In general, the study area presents evident warming, low humidity, and UHI effect.

This study used the buildings within Guangzhou as the land use type for the heat island effect simulation analysis

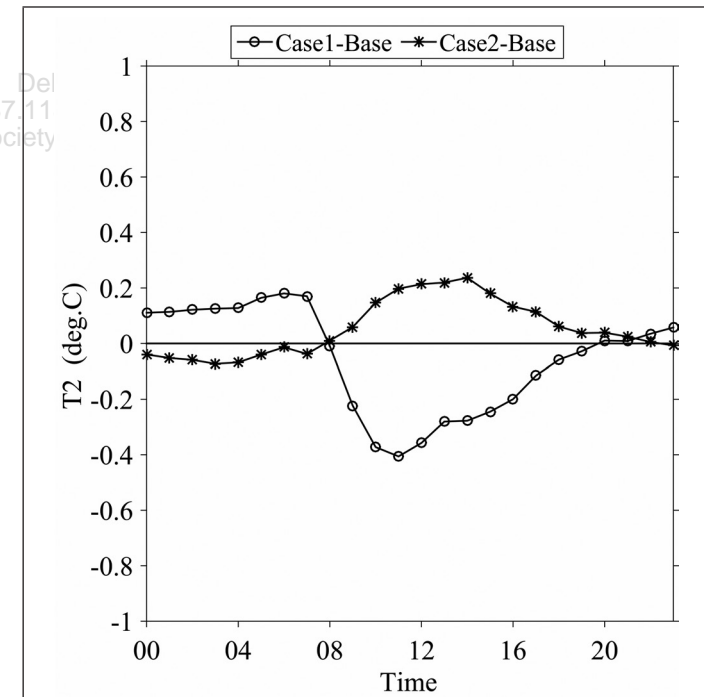


Figure 10(c). Influence of various building densities on the daily variations of the 2 m temperature (T2) in Guangzhou

to verify the effect of various building densities on the heat island effect. This study shows that the higher the high building density, the lower the temperature at daytime and the higher the temperature at nighttime. The lower the density

of buildings, the higher the temperature at daytime and the lower the temperature at nighttime.

The heat island effect is an ecological and environmental problem associated with rapid urbanization. The number of urban buildings pose a substantial impact on the UHI effect. Intensive urban construction will inevitably enhance the city heat island effect. Thus, the urban thermal environment deteriorated, thereby considerably restricting the quality of the urban living environment. The height and density of buildings affect the thermal environment of a city by changing the sunshine and ventilation conditions nearby. However, green land and water with cooling and humidification that regulate the local microclimate and other ecological functions are important controllable factors to ease the heat island effect. Therefore, increasing the layout of urban park green spaces and reducing building density to alleviate the heat island effect in the city is appropriate. Moreover, a high-density building area, with limited land area, green space, and water structure, can be optimized to increase the cooling effect. Such changes can improve the regional thermal environment and urban landscape and provide a substantially comfortable living environment.

Acknowledgments

The authors would like to express their sincere thanks to the journal editor, the guest editors of this special issue, and the two anonymous reviewers for their valuable suggestions and considerate support, who have made this paper possible for publication. This work was supported by the National Natural Science Foundation of China (No. 41271138, 41571118), the Fundamental Research Funds for the Central Universities in China (Ref. 17lg39), the China Special Fund for Meteorological Research in the Public Interest (No. GYHY201406031), and the International Program for Ph.D. Candidates, Sun Yat-Sen University.

References

- Buyantuyev, A., and J. Wu, 2010. Urban heat islands and landscape heterogeneity: Linking spatiotemporal variations in surface temperatures to land-cover and socioeconomic patterns, *Landscape Ecology*, 25:17–33.
- Cenedese A., M.P., 2003. Interaction between an inland urban heat island and a sea-breeze flow: A laboratory study, *Journal of Applied Meteorology*, 11:1569–1583.
- Champollion, C., P. Drobinski, M. Haeffelin, O. Bock, and J. Tarniewicz, 2009. Water vapour variability induced by urban/rural surface heterogeneities during convective conditions, *Quarterly Journal of the Royal Meteorological Society*, 135:1266–1276.
- Connors, J.P., C.S. Galletti, and W.T.L. Chow, 2013. Landscape configuration and urban heat island effects: assessing the relationship between landscape characteristics and land surface temperature in Phoenix, Arizona, *Landscape Ecology*, 28:271–283.
- Freitas, E.D., C.M. Rozoff, W.R. Cotton, and P.L.S. Dias, 2007. Interactions of an urban heat island and sea-breeze circulations during winter over the metropolitan area of São Paulo, Brazil, *Boundary-Layer Meteorology*, 122:43–65.
- Guo, G., Z. Wu, R. Xiao, Y. Chen, and X. Liu, 2015. Impacts of urban biophysical composition on land surface temperature in urban heat island clusters, *Landscape and Urban Planning*, 135:1–10.
- Huang, X., and L. Zhang, 2012. Morphological building/shadow index for building extraction from high-resolution imagery over urban areas, *IEEE Journal of Selected Topics in Applied Earth Observations and Remote Sensing*, 5:161–172.
- Huang, X., and L. Zhang, 2014. A multi-index learning approach for classification of high-resolution remotely sensed images over urban areas, *ISPRS Journal of Photogrammetry and Remote Sensing*, 90:36–48.
- Hussain, M., D. Chen, A. Cheng, H. Wei, and D. Stanley, 2013. Change detection from remotely sensed images: From pixel-based to object-based approaches, *ISPRS Journal of Photogrammetry and Remote Sensing*, 80, 91–106.
- King, V.J., and C. Davis, 2007. A case study of urban heat islands in the Carolinas, *Environmental Hazards*, 4:353–359.
- Kolokotroni, M., and R. Giridharan, 2008. Urban heat island intensity in London: An investigation of the impact of physical characteristics on changes in outdoor air temperature during summer, *Solar Energy*, 82:986–998.
- Kuang, W., Y. Liu, Y. Dou, W. Chi, G. Chen, C. Gao, T. Yang, J. Liu, and R. Zhang, 2015. What are hot and what are not in an urban landscape: Quantifying and explaining the land surface temperature pattern in Beijing, China, *Landscape Ecology*, 30(2):357–373.
- Kusaka, H., 2000. The effects of land-use alteration on the sea breeze and daytime heat island in the Tokyo metropolitan area, *Journal of the Meteorological Society of Japan*, 4:405–420.
- Lang, W., J.D. Radke, T. Chen, and E.H. Chan, 2016a. Will affordability policy transcend climate change? A new lens to re-examine equitable access to healthcare in the San Francisco Bay Area, *Cities*, 58:124–136.
- Lang, W., T. Chen, and X. Li, 2016b. A new style of urbanization in China: Transformation of urban rural communities, *Habitat International*, 55:1–9.
- Luke, H., 1818. *The Climate of London*, W. Phillips.
- Miao, S., F. Chen, M.A. Lemone, M. Tewari, and Q. Li, 2009. An observational and modeling study of characteristics of urban heat island and boundary layer structures in Beijing, *Journal of Applied Meteorology and Climatology*, 3:484–501.
- Mnaley, G., 1958. On tile frequency of snowfall in metropolitan England, *Quarterly Journal of the Royal Meteorological Society*, 84:70–72.
- Oke, T.R., 1982. The energetic basis of the urban heat island, *Quarterly Journal of the Royal Meteorological Society*, 108:1–24.
- Ryu, Y.H., and J.J. Baik, 2012. Quantitative analysis of factors contributing to urban heat island intensity, *Journal of Applied Meteorology and Climatology*, 5, 842–854.
- Sobstyl, J.M., T. Emig, M.A. Qomi, F.J. Ulm, and R.M. Pellonq, 2018. Role of city texture in urban heat islands at nighttime, *Physical Review Letters*, 120(10):108701.
- Sun, R., 2012. How can urban water bodies be designed for climate adaptation?, *Landscape and Urban Planning*, 1:27–33.
- Sun, R., A. Chen, L. Chen, and Y. Lü, 2012. Cooling effects of wetlands in an urban region: The case of Beijing, *Ecological Indicators*, 20:57–64.
- Unwin, D.J., 1980. The synoptic climatology of Birmingham's urban heat island, *Weather* 35:43–50.
- Wu, J., 2014. Urban ecology and sustainability: The state-of-the-science and future directions, *Landscape and Urban Planning*, 125:209–221.
- Zhang, C., H. Tian, S. Pan, M. Liu, G. Lockaby, E.B. Schilling, and J. Stanturf, 2008. Effects of forest regrowth and urbanization on ecosystem carbon storage in a rural-urban gradient in the southeastern United States, *Ecosystems*, 11(8):1211–1222.
- Zhang, C., J. Wu, N.B. Grimm, M. McHale, and A. Buyantuyev, 2013. A hierarchical patch mosaic ecosystem model for urban landscapes: Model development and evaluation, *Ecological Modelling*, 250, 81–100.
- Zhang, T., X. Huang, D. Wen, and J. Li, 2017. Urban building density estimation from high-resolution imagery using multiple features and support vector regression, *IEEE Journal of Selected Topics in Applied Earth Observations and Remote Sensing*, 10, 3265–3280.
- Zhou, W., G. Huang, and M.L. Cadenasso, 2011. Does spatial configuration matter?, Understanding the effects of land cover pattern on land surface temperature in urban landscapes, *Landscape and Urban Planning*, 102, 54–63.